

THE EXCITON MODEL IN MOLECULAR SPECTROSCOPY

M. KASHA, H. R. RAWLS and M. ASHRAF EL-BAYOUMI

Institute of Molecular Biophysics and Department of Chemistry, Florida State University, Tallahassee, Florida

INTRODUCTION

The molecular exciton model has received its most extensive development and application in the field of molecular crystals^{1,2}. More recently, numerous applications to non-crystalline molecular composite systems have been made, including van der Waals and hydrogen-bonded dimers, trimers, and higher order aggregates. Another type of composite system has also been investigated, namely the composite molecule consisting of covalently bonded molecular units, with intrinsic individual unsaturated electronic systems so isolated by single bonds that but little or insignificant electronic overlap between units may occur.

It is now well established that in molecular aggregates and in composite molecules, exciton effects may be observed if sufficiently strong electronic transitions exist in the component sub-units. The result of exciton splitting of excited states in the composite molecule may be the appearance of strong spectral shifts or splittings (which may be of the order of 2000 cm^{-1}) of the absorption bands for the component molecules. At the same time, as a consequence of the exciton splitting of the excited state manifold, an enhancement of triplet state excitation may result.

The purpose of this paper is to present a summary of the various type cases for molecular dimers, trimers and double and triple molecules in the description of the molecular exciton strong-coupling model. Then it will be shown by new experimental examples that, even in those cases where no significant exciton effect is observable in the singlet-singlet absorption spectrum for the composite molecule (intermediate and weak coupling cases), the enhancement of lowest triplet state excitation may still be conspicuous and significant.

The ideas which are summarized in this paper have a curious history. Long ago, Kautsky and Merkel³ demonstrated experimentally that aggregation of dyes facilitated their action as photophysical sensitizers in photochemical reactions, at the same time diminishing their fluorescence efficiency. Kautsky attributed these easily demonstrated effects to enhancement of metastable state excitation in the aggregate dye. There is no doubt today that the metastable state he described is the lowest triplet state of the molecules studied. However, he did not distinguish between intrinsic and enhanced metastable (triplet) state excitation, so his interpretations were largely overlooked. Förster in 1946⁴ used the quasi-classical vector model to

explain the excited state splitting in dye molecule dimers, tentatively suggesting that the metastable lowest *singlet* state resulting for parallel (transition dipole) dimers was the origin of metastable state emission (phosphorescence) in organic molecules. However, after learning of the Lewis and Kasha triplet state studies⁵, Förster in 1949⁶ withdrew entirely his suggestion on the nature of the metastable state and replaced it by the intrinsic molecular (triplet) interpretation instead of the intermolecular (exciton) interpretation. Curiously, both aspects were later recognized as being involved in the enhanced emission properties of dimers. Thus, Levinson, Simpson and Curtis⁷ showed that in a pyridocyanine dimer, fluorescence was quenched, and greatly enhanced triplet-singlet emission was observed, conforming to the excitation paths predicted by a simple exciton splitting for the singlet excited states. McRae and Kasha^{8,9} arrived at the same conclusion as an explanation of some luminescence observations made by Szent-Györgyi on dyes frozen in water-ice¹⁰, and showed that, in general, molecular aggregation could lead to triplet state excitation enhancement by the exciton model. Hoijtink¹¹ has applied the molecular exciton model to the excimer (excited-state stabilized dimer) problem.

THEORETICAL FRAMEWORK

The physical basis of the molecular exciton model¹², the classification of exciton types¹³, and the detailed origin of the theoretical treatment⁹, have been covered in previous papers from this laboratory, in addition to those works cited earlier^{1,2,7,11}. In this section we shall present the simplest skeletal outline of the molecular exciton theory for the case of *molecular dimers* as a complementary paper to those listed above, omitting (electron exchange) anti-symmetrization². The strong coupling case of Simpson and Peterson will be assumed¹⁴.

The molecular exciton model is a state interaction theory. If the intermolecular (interchromophore) electron overlap is small, so that the molecular (chromophore) units preserve their individuality in the composite molecule or aggregate, the molecular exciton model will satisfy the requirements of a perturbation theory. We may then seek solutions (wave-functions and energies) for the aggregate in terms of the wave-functions and energies for the (in our case, electronic) states of the components. The wave-function formalism is rather parallel to molecular orbital theory, but the physical basis and the interpretations are entirely different.

The ground state wave-function of the dimer has the unique description:

$$\Psi_G = \psi_u \psi_v \quad (1)$$

where ψ_u represents the *ground state* wave-function of molecule *u* and ψ_v the corresponding one for molecule *v* (all wave-functions assumed real).

The Hamiltonian operator for the dimer is

$$H = H_u + H_v + V_{uv} \quad (2)$$

where H_u and H_v are the Hamiltonian operators for the isolated molecules, *u* and *v*, and V_{uv} is the intermolecular perturbation potential. The latter is a

coulombic potential, approximated by the point-dipole point-dipole terms of the point-multipole expansion⁹.

The energy of the ground state of the dimer is derivable from the Schrödinger equation as:

$$E_G = \iint \psi_u \psi_v H \psi_u \psi_v d\tau_u d\tau_v \quad (3)$$

which factors into

$$E_G = E_u + E_v + \iint \psi_u \psi_v (V_{uv}) \psi_u \psi_v d\tau_u d\tau_v \quad (4)$$

The last term represents the van der Waals interaction energy (an energy lowering) between the ground states of molecules u and v , and E_u and E_v are the ground state energies of the isolated molecules.

The excited state dimer wave-functions (exciton wave-functions) may be written

$$\Psi_E = r\psi_u^\dagger\psi_v + s\psi_u\psi_v^\dagger \quad (5)$$

where ψ_u^\dagger and ψ_v^\dagger represent *excited state* wave-functions for a particular excited state (with energy E_u^\dagger , E_v^\dagger) under study (u and v assumed identical) of molecules u and v ; and r and s are coefficients to be determined. The Schrödinger equation for the excited state in question is:

$$H(r\psi_u^\dagger\psi_v + s\psi_u\psi_v^\dagger) = E_E(r\psi_u^\dagger\psi_v + s\psi_u\psi_v^\dagger) \quad (6)$$

Multiplying both sides of this equation by $\psi_u^\dagger\psi_v$, and integrating over coordinates for molecules u and v , and repeating this process for $\psi_u\psi_v^\dagger$, leads to two simultaneous equations, containing terms symmetrical in (identical molecule coordinates) u and v :

$$\begin{aligned} H_{uu}(=H_{vv}) &= \iint \psi_u^\dagger\psi_v H \psi_u^\dagger\psi_v d\tau_u d\tau_v \\ H_{uv}(=H_{vu}) &= \iint \psi_u^\dagger\psi_v H \psi_u\psi_v^\dagger d\tau_u d\tau_v \end{aligned} \quad (7)$$

The determinant of the coefficients r and s in these equations is set equal to zero for non-trivial solutions:

$$\begin{vmatrix} H_{uu} - E_E & H_{uv} \\ H_{vu} & H_{vv} - E_E \end{vmatrix} = 0 \quad (8)$$

The roots E_E are, in view of the equivalence of terms in (7):

$$\begin{aligned} E_E' &= H_{uu} + H_{uv} \text{ with } \Psi_E' = \frac{1}{\sqrt{(2)}} (\psi_u^\dagger\psi_v + \psi_u\psi_v^\dagger) \\ E_E'' &= H_{uu} - H_{uv} \text{ with } \Psi_E'' = \frac{1}{\sqrt{(2)}} (\psi_u^\dagger\psi_v - \psi_u\psi_v^\dagger) \end{aligned} \quad (9)$$

Evaluating E_E' and E_E'' by the results in equation (7), we have, owing to the

intrinsic orthonormality conditions for the wave functions for each molecule:

$$\begin{aligned}
 E_E' &= E_u^\dagger + E_v + \int \int \psi_u^\dagger \psi_v (V_{uv}) \psi_u^\dagger \psi_v d\tau_u d\tau_v + \\
 &\quad + \int \int \psi_u^\dagger \psi_v (V_{uv}) \psi_u \psi_v^\dagger d\tau_u d\tau_v \\
 E_E'' &= E_u^\dagger + E_v + \int \int \psi_u^\dagger \psi_v (V_{uv}) \psi_u^\dagger \psi_v d\tau_u d\tau_v - \\
 &\quad - \int \int \psi_u^\dagger \psi_v (V_{uv}) \psi_u \psi_v^\dagger d\tau_u d\tau_v
 \end{aligned} \tag{10}$$

The last term in the equations (10) is the *exciton splitting term*:

$$\mathcal{E} = \int \int \psi_u^\dagger \psi_v (V_{uv}) \psi_u \psi_v^\dagger d\tau_u d\tau_v \tag{11}$$

which in the point-dipole point-dipole approximation becomes⁹

$$\mathcal{E} = \frac{\mathbf{M}_u \cdot \mathbf{M}_v}{r^3} - \frac{3(\mathbf{M}_u \cdot \mathbf{r})(\mathbf{M}_v \cdot \mathbf{r})}{r^5} \tag{11a}$$

and represents an interaction energy due to exchange of excitation energy between molecule u and molecule v . The third term in equations (10) is analogous to the corresponding term in equation (4), and represents the van der Waals interaction (energy lowering) between an excited molecule u and the ground state molecule v .

\mathbf{M}_u is the transition moment in molecule u , and \mathbf{r} is the position vector of the v dipole referred to the u dipole as origin.

If we take the difference of the van der Waals terms of equations (10) and (4) as ΔD , we may give the transition energy for the composite molecule as the differences between equations (10) and equation (4):

$$\Delta E_{\text{composite}} = \Delta E_{\text{unit}} + \Delta D \pm \mathcal{E} \tag{12}$$

This is the characteristic form of the transition energy between states of an aggregate by molecular exciton theory.

As will be evident from equation (12) and from the exciton state energy level diagrams which follow in this paper, the exciton model describes a resonance splitting of the excited state composite molecule energy levels which were non-degenerate in the individual molecule or light-absorbing unit. The ground state is merely displaced by van der Waals interaction compared with the initial molecule ground states.

The molecular exciton wave-functions have the same form as molecular orbital wave-functions, but the dagger represents excitation in the individual molecule, so the nodes are not related to charge distribution as they would be in molecular orbital theory. The nodes in molecular exciton wave-functions correspond to a change in the phase relation of transition dipole. Since mutual phase relations between molecules may be arbitrarily chosen, the interpretation of the nodes in the wave-functions (9) depends on the phase relation convention⁹.

In the following section, a graphical presentation is made of equations (10) for type cases of various composite systems. In the diagram, ΔD is shown relative to a fixed ground state, and the exciton splitting \mathcal{E} is shown as a function of a geometrical parameter for the composite molecule.

EXCITON ENERGY DIAGRAMS FOR COMPOSITE MOLECULES

In this section we shall review some typical simple cases involving small groupings of molecules or light absorbing units. The results will apply equally well to molecular aggregates such as loosely bonded dimers and trimers, or covalently bonded double molecules¹⁵ and triple molecules; to satisfy the application of the exciton model, *electron overlap* between the light absorbing units must be small.

The cases we are dealing with could be described by a detailed quantum mechanical treatment⁹. However, the molecular exciton model lends itself to the applicant of the quasi-classical vector model, since we may approximate the excited state resonance interaction by considering the interaction of transition moment dipoles electrostatically. We shall use this description in this section, which is an elaboration of a previous paper¹⁶.

Parallel transition dipoles in a composite double molecule lead to the exciton energy level diagram shown in *Figure 1*. The ovals correspond to the molecular profile, and the double arrow indicates the polarization axis for the molecular electronic transition considered (the long molecular axes need not be parallel to the transition polarization axis). To the right of the exciton states E' and E'' are indicated the vector diagrams which permit (separately) the evaluation qualitatively of (i) the *energy* of the exciton splitting \mathcal{E} , and (ii) the *transition moments* M measuring the transition probability between the ground state and the exciton states E' and E'' of the composite molecule.

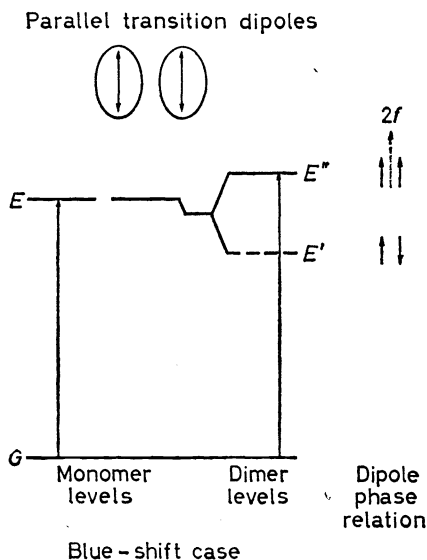


Figure 1. Exciton band energy diagram for a molecular dimer, or a double molecule, with parallel transition dipoles

The out-of-phase dipole arrangement corresponds electrostatically to a lowering of energy (\mathcal{E} negative), so E' lies lower than the van der Waals displaced states of the component molecules; and the in-phase dipole interaction gives repulsion, so \mathcal{E} is positive, and E'' is displaced upwards from the displaced origin. The transition moment is given by the vector sum

THE EXCITON MODEL IN MOLECULAR SPECTROSCOPY

of the individual transition dipole moments in the component molecule. Thus, transitions from the ground state to exciton state E' are forbidden, while transitions from the ground state to exciton state E'' are allowed (oscillator strength $2f$ /dimer, or no change in oscillator strength predicted per monomer concentration, in the present approximation; actually hypo- and hyperchromic effects are found and predicted in a higher order approximation^{17,18}). As mentioned earlier, Förster used this type of discussion for

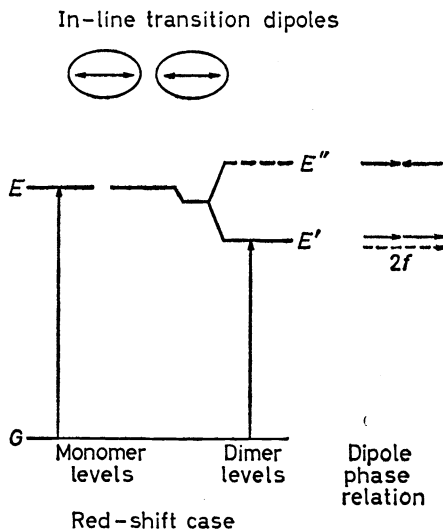


Figure 2. Exciton band energy diagram for a molecular dimer, or a double molecule, with in-line transition dipoles

dye-dimer excited states in a tentative explanation of metastable state formation in molecules.

There are two physical consequences of the exciton splitting which may be observed spectroscopically. The first is immediately obvious from the diagram (*Figure 1*), namely, that the singlet-singlet electronic transition in the dimer will be blue-shifted with respect to that in the monomer; the blue shifts are calculated to be quite large for strongly absorbing monomer units, such as dye molecules^{7,9}. The second consequence of the exciton band formation is not quite as apparent: that enhancement of lowest triplet state excitation will occur in the dimer, accompanied by a quenching of the fluorescence. We shall return to this problem at the end of this section since it involves the triplet electronic states of the molecules which have been omitted from the diagram in *Figure 1*.

Figure 1 corresponds to one of the most frequently occurring van der Waals dimers, the London-force dimer between planar conjugated molecules. Dimers of this type have been widely studied and invariably exhibit a blue shift in the range $1000\text{--}2500\text{ cm}^{-1}$, accompanied by a characteristic fluorescence quenching. It is interesting that as one studies theoretically the further aggregation of the dye into the long thread-like polymers, the exciton model predicts that the band splitting will be about 2.4 times the splitting observed for the dimer⁹. Extensive experimental studies¹⁹ in

the field of spectra of dyes absorbed on polymers, as well as spectra of dyes absorbed on cellular surfaces (in cytological staining), conform to this description of the dye molecule adsorbed as dimer or as polymer. Thus, the phenomena of metachromatias of adsorbed dye are understandable in terms of the exciton model.

In-line transition dipoles in a composite double molecule lead to the exciton energy level diagram shown in *Figure 2*. As before, the polarization axis for the electronic transition under study in the unit molecule is shown aligned with the long axis of the molecule represented in oval profile; however, a more frequent case of in-line transition dipoles would occur for the long geometrical axes of the molecule parallel, but with transition dipoles polarized along the short axis of a unit molecule (in-line in the dimer).

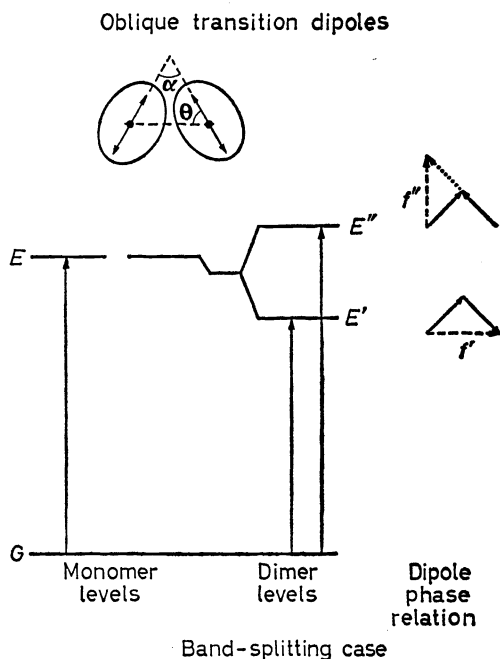


Figure 3. Exciton band energy diagram for a molecular dimer, or a double molecule, with oblique transition dipoles

Again we may use the quasi-classical vector model to analyse the energy of the exciton states produced in the dimer, as well as the transition moment for transitions from the ground state to the resultant exciton states. From the diagram it is readily seen that the in-phase arrangement of transition dipoles leads to an electrostatic attraction, producing the excited state E' of *Figure 2*, whereas the out-of-phase arrangement of transition dipoles causes repulsion, producing the state E'' . On the other hand, the transition moments are finite for electric dipole transitions from the ground state to E' , and 0 to the state E'' from the ground state.

Thus, it will be apparent that the in-line transition dipole case will lead to the observation of a strong spectral red shift for the transition in the dimer

or double-molecule compared with that for a monomer. A number of experimental examples of this type of dimer are known.^{18,9}

Oblique transition dipoles in a composite double molecule lead to the exciton energy diagram shown in *Figure 3*. In this case, the in-phase arrangement of transition dipoles for the monomer is attractive and leads to a lowering of energy, and the out-of-phase arrangement of transition dipoles is repulsive and causes a raising of the excited state energy for the composite molecule. The transition moments for electric dipole transitions from the ground state to the exciton states of the dimer are in this case both non-vanishing. Characteristic of the exciton model, we find that the oscillator strengths f' and f'' for transitions to the two exciton states are polarized mutually perpendicularly.

The exciton splitting energy, corresponding to the separation $\Delta \mathcal{E} = E'' - E'$, is given by:

$$\Delta \mathcal{E} = \frac{2|\mathbf{M}|^2}{r_{uv}^3} (\cos \alpha + 3 \cos^2 \theta) \quad (13)$$

where \mathbf{M} is the transition moment for the singlet-singlet transition in the monomer, r_{uv} is the centre to centre distance between molecules u and v , α is the angle between polarization axes for the component absorbing units and θ is the angle made by the polarization axes of the unit molecule with the line of molecular centres. The transition moments to the exciton states E' and E'' are given by:

$$\begin{aligned} \mathbf{M}' &= \sqrt{2\mathbf{M} \cos \theta} \\ \mathbf{M}'' &= \sqrt{2\mathbf{M} \sin \theta} \end{aligned} \quad (14)$$

where the symbols are as defined for equation (13).

A characteristic feature of exciton theory is illustrated by equation (13). It is seen that the exciton splitting energy is directly related to the square of the transition moment for the component molecules. Thus, the greater the intensity of light absorption in the unit molecule, the greater is the exciton band splitting. The square of the transition moment \mathbf{M} is a measure of the oscillator strength f for the transition.

Another characteristic feature of exciton theory is the dependence of the exciton splitting on the inverse cube of the intermolecular distance r_{uv} . Finally, the geometrical parameters enter in the manner characteristic of the structure of the composite molecule.

Equations (13) and (14) apply equally well to *Figures 1, 2, and 3* with a selection of suitable parameters. It may be mentioned that to apply *Figure 3* to an experimental case, one would generally speaking, have to consider a hydrogen-bonded dimer which could fix the transition moment axes in an oblique orientation. To date no experimental examples of such a hydrogen-bonded dimer have been studied, although there are numerous possibilities.

Coplanar inclined transition dipoles in a composite molecule lead to the exciton energy diagram shown in *Figure 4*. This case covers continuously the variation of angle θ between polarization axes and the line of molecule centres. Thus, 0 degrees corresponds to *Figure 2* and 90 degrees corresponds to *Figure 1*, covering our previous cases.

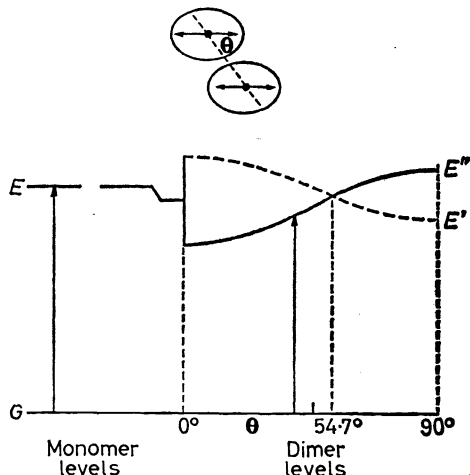


Figure 4. Exciton band energy diagram for a molecular dimer, or a double-molecule, with coplanar transition dipoles inclined to interconnected axis by angle θ

The exciton band splitting in this case is given by the formula^{8,9}:

$$\Delta \mathcal{E} = \frac{2|\mathbf{M}|^2}{r_{uv}^3} (1 - 3 \cos^2 \theta) \quad (15)$$

with the symbols as previously defined. It is evident that for the value of $\theta = \arccos 1/\sqrt{3} = (54.7^\circ)$, the exciton splitting is zero, *i.e.*, the dipole-dipole interaction is zero for this orientation of transition moments in the component molecules, irrespective of intermolecular distance r_{uv} .

Non-planar transition dipoles

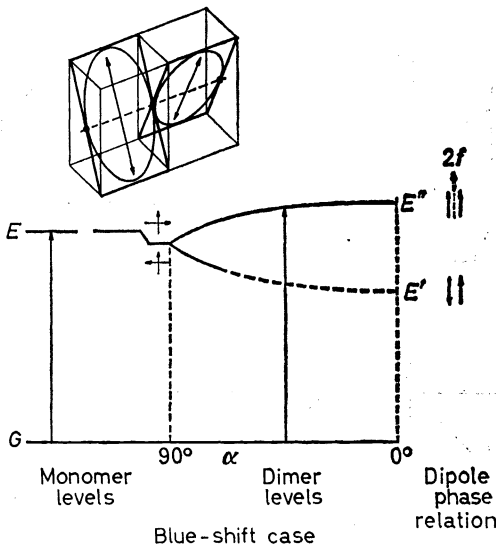


Figure 5. Exciton band energy diagram for a molecular dimer, or a double molecule, with non-coplanar transition dipoles with angle α between molecular planes

The transition moments for this case are given⁹ by $\mathbf{M}' = 0$ and $\mathbf{M}'' = 2\mathbf{M}$, where \mathbf{M} is the electric dipole transition moment for the transition under study in the component molecule, \mathbf{M}' and \mathbf{M}'' correspond to the out-of-phase and in-phase arrangement of transition dipoles corresponding to the labelling of exciton states E' and E'' of Figure 4. Equation (15) and the discussion of transition moments in this paragraph, apply equally well to Figures 1 and 2, with a selection of suitable parameters.

Figure 4 illustrates a common type of exciton band energy diagram wherein an exciton state forbidden for excitation by electric dipole radiation interchanges position on the energy level diagram with an allowed exciton state, as a function of geometry of the aggregate.

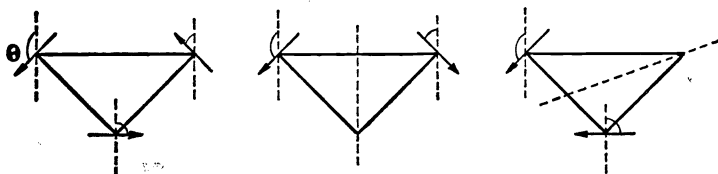
Non-planar transition dipoles in the composite double molecules lead to the exciton energy diagram shown in Figure 5. This case may be considered as another geometrical variation of the parallel transition dipole case of Figure 1. The exciton splitting energy in this case is given by:

$$\Delta \mathcal{E} = \frac{2|\mathbf{M}|^2}{r_{uv}^3} (\cos \alpha - 3 \cos^2 \theta) \quad (16)$$

where α is the angle between the two molecular planes defined by the diagram in Figure 5 and θ is the angle between the polarization axes and the line of molecular centres. The transition moments for electric dipole transitions from the ground state to the two exciton states E' and E'' vary continuously with angle α . The vector diagrams show the phase relationship between transition dipoles for the two extreme values of angle α .

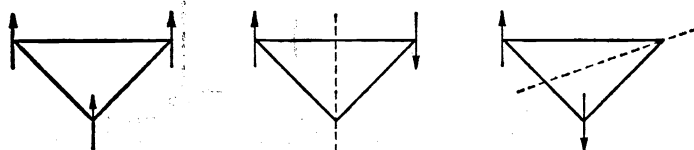
In particular, the case of the out-of-phase dipole array leads to a progressively more allowed exciton state as the angle α approaches 90 degrees

Cyclic trimer transition dipole arrays



Dipole phase relations for in-plane arrays

(Angle θ indicates rotation convention for out-of-plane correlation)



Dipole phase relations for out-of-plane arrays

Figure 6. Transition dipole vector diagrams for exciton model of cyclic trimer or cyclic triple molecule

(for electric dipole transitions from the ground state). If the diagram were continued to 180 degrees in α , it would of course be symmetrical and would feature a lowest exciton state which always has some forbidden character. This is a feature we shall meet again for composite triple molecules.

Cyclic trimer transition dipole arrays in a composite triple molecule are diagrammed by the vector model in *Figure 6*. Each apex of the triangle corresponds to a component molecule or light-absorbing unit, with transition dipoles designated by an arrow. The lowest exciton wave-function (for in-plane arrays, upper half of *Figure 6*) is taken as nodeless, with transition dipoles in phase. For a figure with a threefold axis of symmetry, the next exciton wave-functions are doubly degenerate. Thus, *Figure 6* shows a similar pair of one-noded vector diagrams corresponding to single-noded exciton wave-functions. The node corresponds to a change of phase relation in the transition dipole as one goes around the triangle. For convenience, the node has been chosen through the apex in both cases. It is clear that for the in-plane array the nodeless wave-function corresponds to the lowest energy exciton state, while the single-noded degenerate wave-functions correspond to repulsive exciton states. On the other hand, the nodeless wave-function corresponds to an exciton state which is forbidden with respect to electric dipole transitions from the ground state, while the doubly degenerate arrays correspond to allowed exciton states for electric dipole transitions.

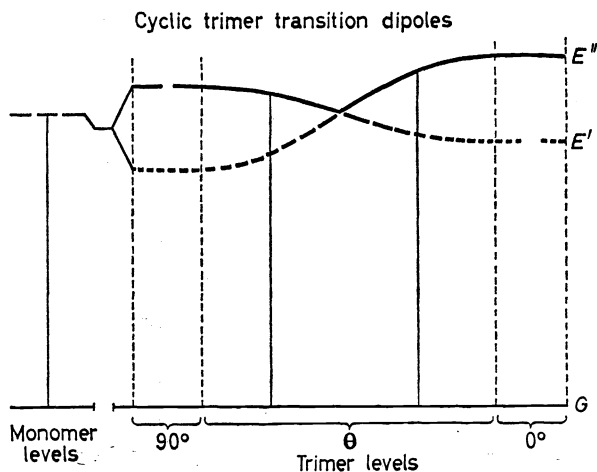


Figure 7. Schematic exciton band energy diagram for a cyclic trimer or a cyclic triple molecule (cf. *Figure 6* for phase relations and angle of rotation)

Out-of-plane arrays can be considered analogously, corresponding to the lower half of *Figure 6*. Angle θ measures the angle between the component transition dipoles and the normal to the plane of the trimer array at the triangle apex. By variation of the angle θ , one may correlate the vector diagrams for the in-plane dipole arrays with those out-of-plane dipole arrays. This correlation leads to the exciton energy level diagram depicted in *Figure 7*.

In the monomer the excited states under study are triply degenerate by definition. In the 90 degree trimer array the upper exciton state is doubly

degenerate and allowed (for electric dipole transitions from the ground state) and the lower exciton state is non-degenerate and forbidden (correspondingly). In the 0 degree trimer array, the upper exciton state is non-degenerate and allowed (for electric dipole transitions from the ground state), while the lower exciton states are doubly degenerate and forbidden (correspondingly).

Thus we see in *Figure 7* that the triple degeneracy of the three monomer units is only partially split in the exciton diagram of the trimer and, moreover, the lower exciton state always has some forbidden character and at the extreme limits of $\theta = 0$ and 90 degrees, the lower exciton states are completely forbidden for excitation by electric dipole radiation. This forbidden character of the lower exciton state will have a profound effect on the excitation pathways in trimeric composite molecules.

Excitation pathways for exciton diagrams in composite molecules are typified by the diagram shown in *Figure 8* for the parallel transition dipole dimer case⁷⁻⁹. In the monomer, absorption is taken as strongly allowed for electric dipole radiation. Fluorescence will then be commonly observed under favourable conditions. On the other hand, phosphorescence in such cases will be of limited intrinsic quantum efficiency. Such excitation properties are commonly found in many dye molecules and other polyatomic molecules with $\pi - \pi^*$ electron transitions.

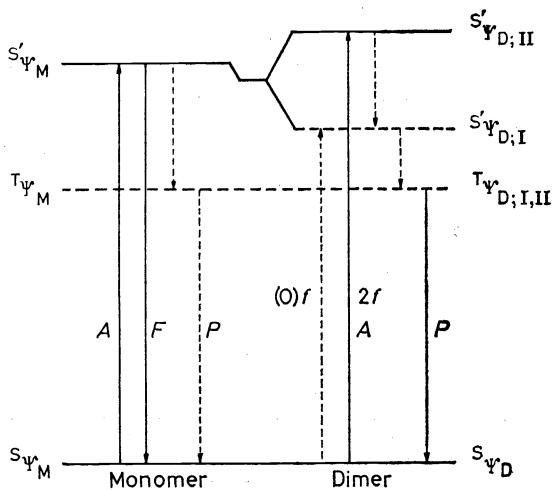


Figure 8. Paths of excitation between singlet and triplet states without and with exciton splitting (parallel transition dipole dimer case)

In the composite molecule, considering the most favourable case for our discussion, in which the lower exciton state is forbidden, we have the probable pathways as shown on the right side of *Figure 8*. Here absorption to the lower exciton state is forbidden, whereas absorption to the upper exciton state is still strongly allowed.

Since the exciton splitting depends on the oscillator strength of the transition, only the singlet states of the composite molecules are split in a gross fashion. The triplet states of the monomer will remain nearly degenerate in the composite molecule and are shown as unsplit in the diagram.

After excitation to the allowed upper exciton singlet state of *Figure 8*, the rapid *internal conversion* between singlet states may be expected to completely prevent the fluorescence from the allowed exciton state (back to the ground state), so that the forbidden exciton state will not be excited with high efficiency. Radiative transitions from the lower exciton state to the ground state are formally forbidden (distortions in the aggregate geometry may lead to a small probability of transition, corresponding to lifetimes in the millisecond range). Consequently, the radiationless intersystem crossing process, which has rate constants on the order of 10^7 sec^{-1} , may be expected to be the important next step, leading to highly efficient triplet excitation in this dimer. Finally, phosphorescence or triplet state emission in the composite molecule may be expected to proceed with relatively high efficiency.

The pathways of excitation described above were proposed by Levinson, Simpson and Curtis⁷ in their studies of pyridocyanine dimers and by McRae and Kasha^{8,9} in their studies of luminescence in molecular aggregates. The descriptions given correspond to the common observation that London-force parallel dimers of dye molecules exhibit a complete quenching of fluorescence of the monomer, and a corresponding great increase in the phosphorescence quantum efficiency.

We may thus expect enhanced lowest triplet state excitation in composite molecules which exhibit exciton splitting of lowest singlet excited states, especially when the lowest exciton state assumes a forbidden character with respect to radiative transitions.

TRIPLET EXCITATION ENHANCEMENT IN COMPOSITE MOLECULES

In this section we shall present an experimental study of triplet state excitation enhancement as a consequence of exciton splitting phenomena. The cases considered here will be covalently bonded composite molecules such as the aryl methanes and aryl amines. It will be shown that even in cases where the exciton splitting is quite small, so that the weak or intermediate coupling exciton model^{14,16} applies, triplet state excitation enhancement is nevertheless demonstrable. In such cases the exciton splitting will hardly be observable in low resolution solution spectra, but owing to the greater sensitivity of luminescence methods, a gross effect on the phosphorescence fluorescence quantum yield ratio may be observed. Although some previous studies have been made on the exciton effect in some of these molecules in high resolution 20°K absorption spectra of crystals^{20,21}, no luminescence studies related to the exciton splitting phenomenon have been previously reported for these molecules. Our discussion will be qualitative and will relate to the exciton energy level diagrams of the previous section.

Diphenylmethane and triphenylmethane offer a clear-cut example of the triplet state enhancement through exciton splitting. Diphenylmethane is pictured in *Figure 9* in a two-fold axis geometry. Diphenylmethane may be considered²⁰ as a covalent dimer of toluene, for which the lowest absorption band has molar absorption coefficient of approximately $\epsilon = 200$. The lowest singlet excited state of toluene is of L_b type and is polarized along the short axis of the molecule by a factor of 2 over long axis polarization²¹ (long axis is the $\text{CH}_n\text{-phenyl}$ axis). McClure assumed²⁰ that the $\text{C}-\text{CH}_2-\text{C}$ angle in

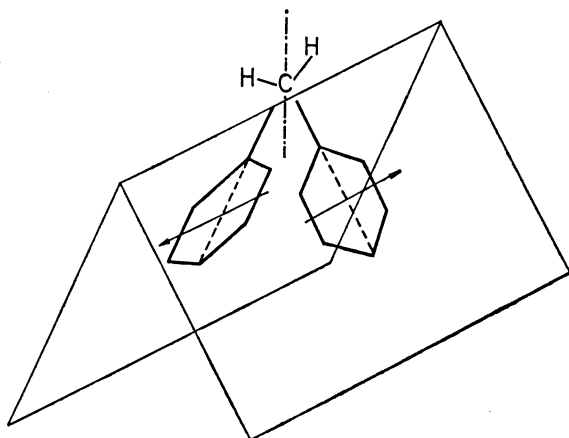


Figure 9. Diphenylmethane as a double molecule, showing vertical two-fold axis and symmetric phase relation of transition dipoles for two-fold rotation

diphenylmethane is about 112 degrees, close to the tetrahedral angle. He then calculated the exciton splitting as a function of the angle of rotation ϕ of the phenyl groups about the C—C bond, measured from the perpendicular position. McClure also calculated the transition moment to each of the two exciton states, and concluded that the higher state always has the higher transition moment. McClure's formula (corrected) for the exciton splitting in diphenylmethane is:

$$\Delta \mathcal{E} = \frac{2|\mathbf{M}|^2}{r_{uv}^3} (2.308 \sin^2 \phi - 1) \quad (17)$$

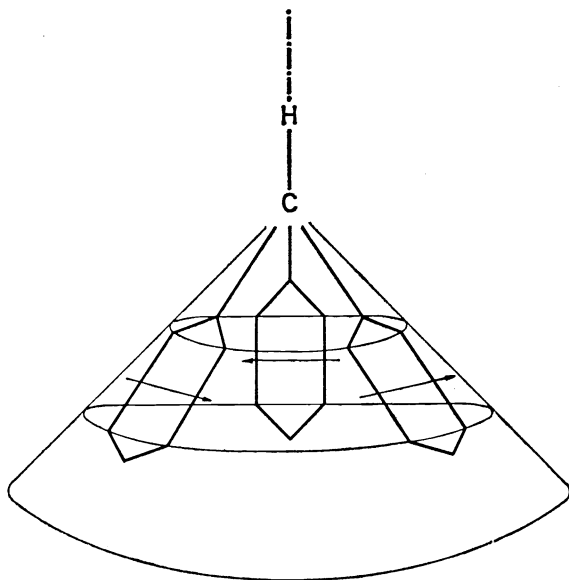


Figure 10. Triphenylmethane as a triple molecule, showing vertical three-fold axis and symmetric phase relation of transition dipoles for three-fold rotation

where the ϕ is taken to be 0 for the phenyl rings perpendicular to the C—CH₂—C plane, and the rotation of the two rings is taken in-phase; the C—CH₂—C apex angle was assumed to be 112°. The spectral results in the crystal indicated that ϕ is approximately 30° in diphenylmethane. An angle

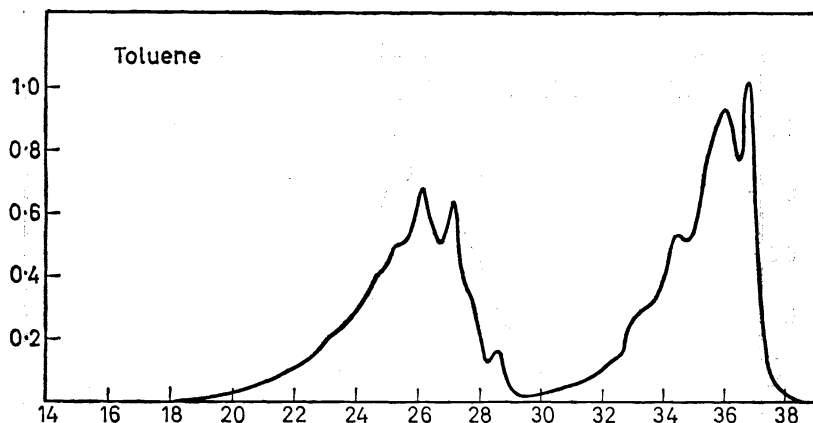


Figure 11. Total luminescence spectrum of toluene in EPA rigid glass solution at 77°K. Singlet-singlet emission (fluorescence) on right. Triplet-singlet emission (phosphorescence) on left. Corrected emissivity curves, ordinate: arbitrary intensity units; abscissa: wavenumbers $\times 10^{-3}$

of 0° would correspond in principle to an exciton band energy diagram of the type shown in Figure 1, with excitation paths described in Figure 8. McClure's exciton band energy diagram for diphenylmethane is of a type analogous to our Figure 5, except that his two exciton states cross at $\phi = 41^\circ$.

Thus, in diphenylmethane, the lower exciton component has some forbidden character, and an enhancement of lowest triplet excitation would be expected.

Triphenylmethane is pictured in Figure 10 in a three-fold axis geometry. We may anticipate that qualitatively the exciton band energy diagram for

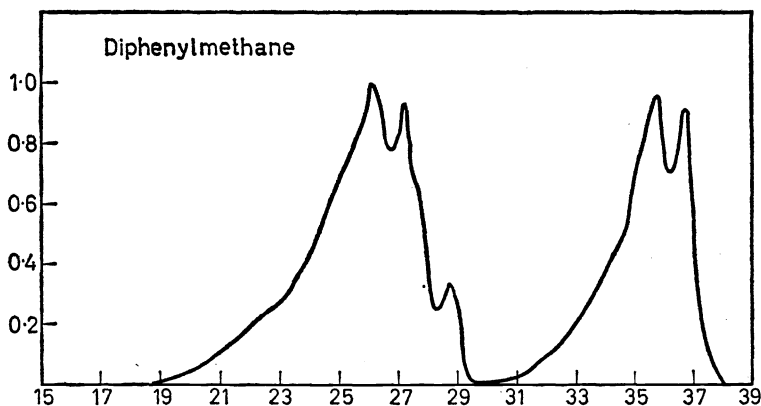


Figure 12. Total luminescence spectrum of diphenylmethane in EPA rigid glass solution at 77°K. Singlet-singlet emission (fluorescence) on right. Triplet-singlet emission (phosphorescence) on left. Corrected emissivity curves, ordinate: arbitrary intensity units; abscissa: wavenumbers $\times 10^{-3}$

THE EXCITON MODEL IN MOLECULAR SPECTROSCOPY

this molecule may conform to the diagrams of *Figures 6 and 7*, although the apex angle correction would alter the quantitative results to a degree. Thus, in this case also, an enhancement of triplet state excitation would be anticipated from the diagrams, in reference to the excitation paths of *Figure 8*, for a lowest singlet-exciton level of forbidden character.

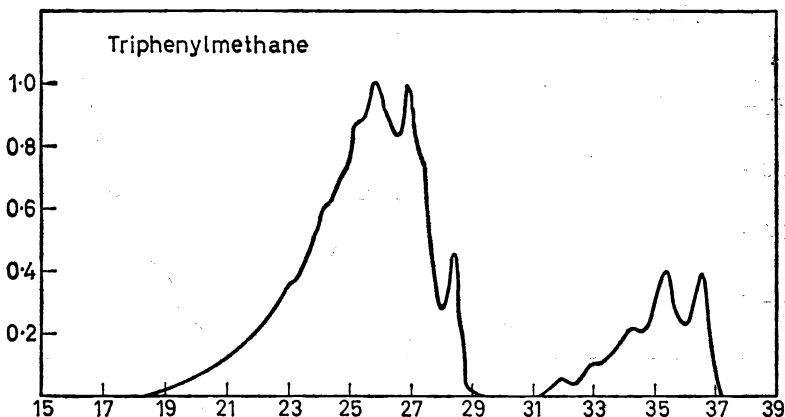


Figure 13. Total luminescence spectrum of triphenylmethane in EPA rigid glass solution at 77°K. Singlet-singlet emission (fluorescence) on right. Triplet-singlet emission (phosphorescence) on left. Corrected emissivity curves, ordinate: arbitrary intensity units; abscissa: wavenumbers $\times 10^{-3}$

The experimental results for *toluene*, *diphenylmethane*, and *triphenylmethane* are shown in *Figures 11, 12, and 13*, and are numerically summarized in *Table 1*. It is seen that the phosphorescence-fluorescence ratio increases conspicuously in this series, while at the same time the phosphorescence mean lifetime remains relatively constant.

Table 1. Intersystem crossing enhancement in composite molecules (hydrocarbons)

<i>Molecule</i>	<i>Intersystem crossing ratio, Φ_P/Φ_F</i>	<i>Mean lifetime, τ_P (sec)</i>
Toluene	0.94	8.8
Diphenylmethane	1.46	9.4
Triphenylmethane	4.12	7.9

It is interesting that a decrease in fluorescence to the advantage of phosphorescence would not be predictable from the kinetic analysis²² of excitation paths if exciton interaction were neglected. Thus, the lowest singlet-singlet absorption band in toluene ($\log \epsilon = 2.3$), in diphenylmethane²³ ($\log \epsilon = 2.7$), and in triphenylmethane²⁴ ($\log \epsilon = 2.9$) becomes progressively stronger; this would suggest that the fluorescence lifetime should decrease, and that fluorescence should compete progressively more favourably in this series. The fact that the opposite is the case requires a novel explanation, which is provided by the exciton model.

An alternative explanation might have been possible if a spin-orbital

perturbation enhancement from some upper state interaction in the composite molecule had occurred. But the near constancy of the triplet state lifetimes (*Table 1*) clearly indicates that the spin-orbital perturbation is nearly unaffected by the formation of the composite molecule.

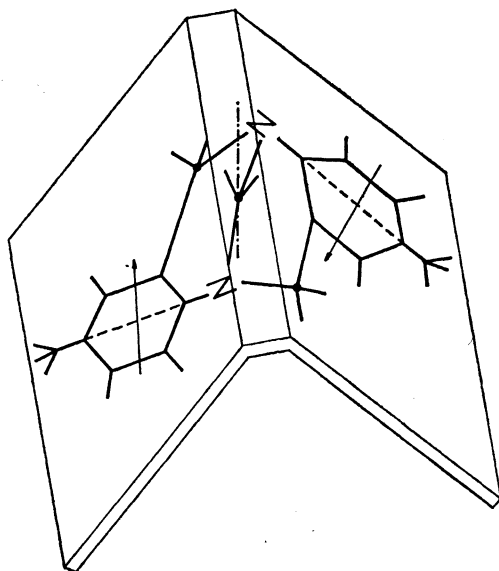


Figure 14. Tröger's base as a double molecule, showing vertical twofold axis and symmetric phase relation of transition dipoles for two-fold rotation

The *aromatic amines* are more complex to deal with than are the corresponding aromatic hydrocarbons because another phenomenon complicates the luminescence behaviour of these molecules. In a separate study²⁵ it is shown that the presence of intramolecular charge transfer transitions ($l \rightarrow a_\pi$ type²⁶) in these molecules leads to enhancement of triplet state excitation in comparison with a related hydrocarbon. Nevertheless, as an overlay there is also demonstrable an additional triplet state excitation enhancement in composite molecules made of aromatic amine component molecules.

Tröger's base is depicted in *Figure 14* as a double molecule, with two covalently bonded *N,N*-dimethylanilines held in a C_2 geometry. In *Figure 15*

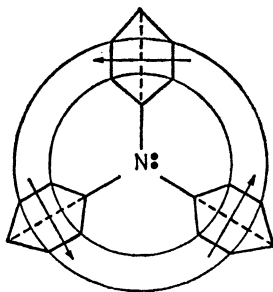


Figure 15. Triphenylamine as a triple molecule, showing planar conformation with symmetric phase relation of transition dipoles for rotation about normal three-fold axis

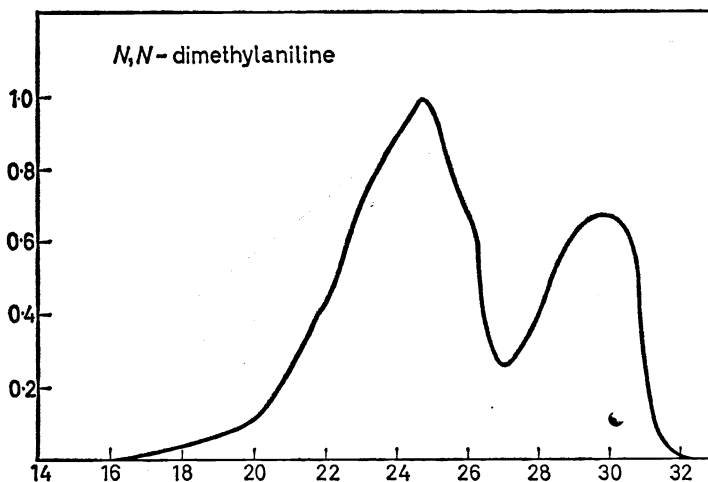


Figure 16. Total luminescence spectrum of *N,N*-dimethylaniline in EPA rigid glass solution at 77°K. Singlet-singlet emission (fluorescence) on right. Triplet-singlet emission (phosphorescence) on left. Corrected emissivity curves, *ordinate*: arbitrary intensity units; *abscissa*: wavenumbers $\times 10^{-3}$

triphenylamine is depicted as a triple molecule, with three phenyls arranged about the N atom in a D_{3h} geometry.

The luminescence spectra of *N,N*-dimethylaniline, Tröger's base, and *o*-*N,N*-dimethyltoluidine are presented in Figures 16, 17 and 18, with corresponding numerical data in Table 2.

The luminescence spectra of *diphenylamine* and *triphenylamine* are presented in Figures 19 and 20, with data again summarized in Table 2.

Tröger's base is a rather rigid structure, with the angle between transition moments being approximately 18 degrees for short axis polarization (Figure 14). Qualitatively, the exciton band energy diagram will approximate

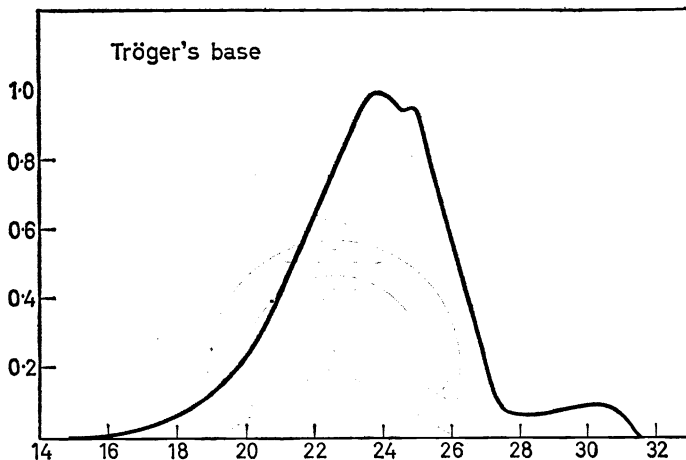


Figure 17. Total luminescence spectrum of Tröger's base in EPA rigid glass solution at 77°K. Singlet-singlet emission (fluorescence) on right. Triplet-singlet emission (phosphorescence) on left. Corrected emissivity curves, *ordinate*: arbitrary intensity units; *abscissa*: wavenumbers $\times 10^{-3}$

Figure 1, and a very considerable enhancement of triplet state excitation may be expected. The data of Table 2 confirm this expectation.

Table 2. Intersystem crossing enhancement in composite molecules (aromatic amines)

Molecule	Intersystem crossing ratio, Φ_P/Φ_F	Mean lifetime, τ_P (sec)
<i>N,N</i> -dimethylaniline	2.01	2.8
Tröger's base	18.8	1.9
<i>o-N,N</i> -dimethyltoluidine	2.38	2.3
Diphenylamine	3.26	2.1
Triphenylamine	8.31	0.74

Comparing *N,N*-dimethylaniline, diphenylamine, and triphenylamine, the data of Table 2 and the corresponding figures indicate a pronounced enhancement of triplet state excitation in this series. A comparison of the data of Table 2 with that of Table 1 shows the enhancement effect for triplet excitation of the aromatic amines relative to the corresponding hydrocarbon, owing to the intramolecular charge transfer state interaction²⁵ (the small phosphorescence lifetime variations reflect this). However, the composite molecule effect is still clearly evident for the aromatic amine series.

The oscillator strengths for the lowest singlet-singlet absorption are 0.027 for aniline, 0.19 for diphenylamine, and 0.25 for triphenylamine (methylcyclohexane solvent, 20°C). As in the case of the corresponding aromatic hydrocarbon series, these data would require a decrease of fluorescence lifetime, with a corresponding decrease in the phosphorescence/fluorescence quantum yield ratio for the series. The composite molecule effect through the exciton model seems to be a necessary explanation in this case also.

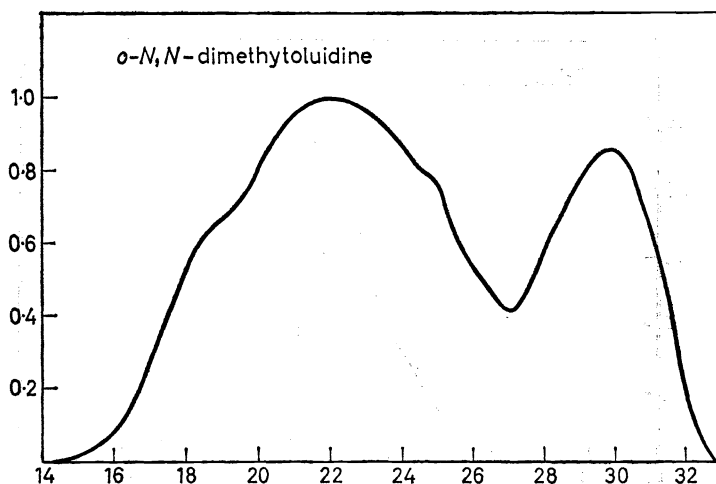


Figure 18. Total luminescence spectrum of *o-N,N*-dimethyltoluidine in EPA rigid glass solution at 77°K. Singlet-singlet emission (fluorescence) on right. Triplet-singlet emission (phosphorescence) on left. Corrected emissivity curves, ordinate: arbitrary intensity units; abscissa: wavenumbers $\times 10^{-3}$

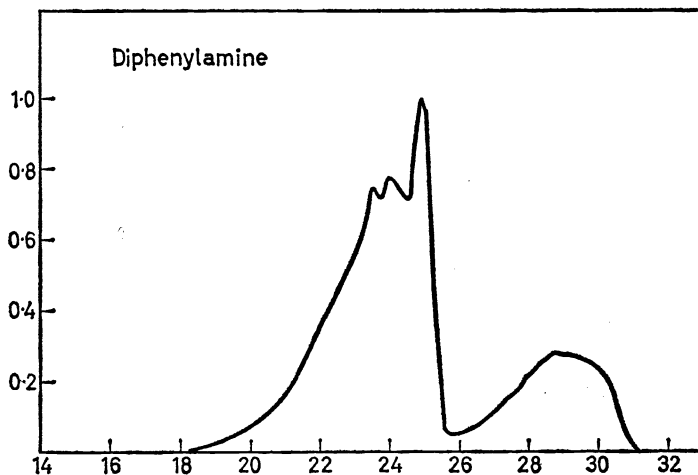


Figure 19. Total luminescence spectrum of diphenylamine in EPA rigid glass solution at 77°K. Singlet-singlet emission (fluorescence) on right. Triplet-singlet emission (phosphorescence) on left. Corrected emissivity curves, ordinate: arbitrary intensity units; abscissa: wavenumbers $\times 10^{-3}$

In all of the experimental cases studied low temperature (77°K) rigid glass spectroscopy was used. An important point to emphasize is the *temperature-dependent* nature of the phenomenon we have described. If these had been strong-coupling cases, the absorption spectral effects would have been very conspicuous, and the excitation behaviour would have been relatively temperature independent⁸. However, here the absorption spectral effects are virtually unnoticeable. Thus, the two exciton levels (the more strongly allowed upper one, and the relatively forbidden lower one, whose existence facilitates the phosphorescence enhancement) must be relatively close

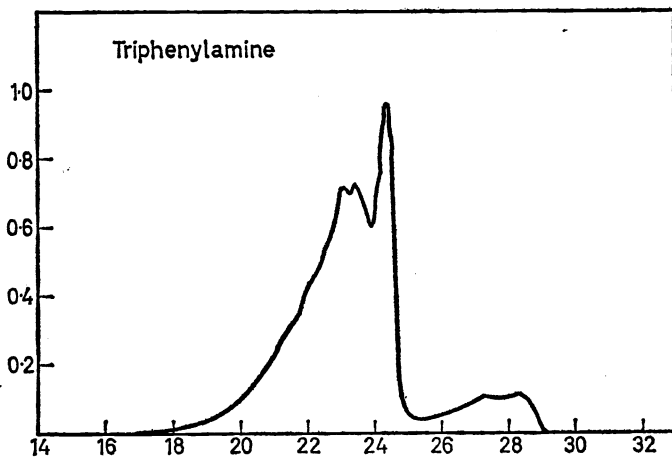


Figure 20. Total luminescence spectrum of triphenylamine in EPA rigid glass solution at 77°K. Singlet-singlet emission (fluorescence) on right. Triplet-singlet emission (phosphorescence) on left. Corrected emissivity curves, ordinate: arbitrary intensity units; abscissa: wavenumbers $\times 10^{-3}$

together. Probably, in most of the molecules we have studied, the exciton splitting is of the order of kT at room temperature. Under these conditions, the triplet state enhancement would become progressively more prominent as one lowered the temperature. *A study of such temperature dependence triplet state enhancement in composite molecules could serve to give data on exciton splitting in weak coupling cases, a datum otherwise difficult to obtain.*

As an experimental note, we indicate a few essential points on the data handling for *Figures 11–13 and 16–20*. The emission spectra were recorded with a Perkin–Elmer Model 99 recording double-pass monochromator using fused quartz optics and an RCA 1P-28 photomultiplier. A Bausch and Lomb grating monochromator (0.5 m F.L.) with a G.E. AH-6 high-pressure mercury arc or a Hanovia high-pressure mercury–xenon arc were used for excitation. The spectrometer–photomultiplier correction was determined by recording the emissivity from a standard lamp provided by the National Bureau of Standards, with conversion of data to quanta per wavenumber interval. The correction factor so determined was applied to all of the emission curves presented. The data of *Tables 1 and 2* were then obtained by graphical integration of the corrected curves.

Summarizing our presentation, we emphasize that molecular luminescence studies, by their greater selectivity and sensitivity, may be used to detect weak interactions in molecular composite systems, even when such interactions are not detectable in low-resolution absorption studies. Our demonstration of triplet state enhancement in composite molecules suggests important photochemical applications. Instead of using perturbation methods (*e.g.*, heavy atom substituents, or heavy atom environmental effects), triplet state excitation may be increased significantly by building up a composite molecule whose individual units are of interest for photochemical investigation. The expected temperature dependence for weak coupling cases adds a new experimental parameter.

CONCLUSION

The molecular exciton model, which deals with the excited state resonance interaction in weakly coupled electronic systems, has been described as an interpretative tool for the study of the spectra and photochemistry of composite molecules. Under composite molecules are grouped loosely bound groups of light-absorbing units, held together by hydrogen bonds or by van der Waals forces. Another group of composite molecules included in the study consists of covalently bound light-absorbing units.

A skeletal outline of the simplest quantum mechanical framework for the description of the model has been presented. A series of explicit exciton splitting formulae has been given for various geometrical arrangements of double molecules, accompanied by the characteristic exciton splitting diagrams and vector model analogues.

As an example of composite molecule effects on molecular excitation, a comparison has been made between the spectral properties of toluene, diphenylmethane and triphenylmethane, with an analogous comparison for aniline, diphenylamine and triphenylamine.

It has been shown that in composite molecules a significant triplet state

THE EXCITON MODEL IN MOLECULAR SPECTROSCOPY

excitation enhancement results from the exciton interaction among excited states of the component molecules. Applications to photochemical interpretations have been discussed.

We are pleased to acknowledge with thanks a gift of some aromatic amines by Professor B. M. Wepster of the University of Delft, Holland, which made the completion of our study possible.

References

- ¹ A. S. Davydov. *Theory of Molecular Excitons* (translated by M. Kasha and M. Oppenheimer, Jr.). McGraw-Hill, New York (1962).
- ² D. S. McClure. *Electronic Spectra of Molecules and Ions in Crystals*. Academic Press, New York (1959).
- ³ H. Kautsky and H. Merkel. *Naturwissenschaften* **27**, 195 (1939).
- ⁴ Th. Förster. *Naturwissenschaften* **33**, 166 (1964).
- ⁵ G. N. Lewis and M. Kasha. *J. Am. Chem. Soc.* **66**, 2100 (1944).
- ⁶ Th. Förster. *Naturwissenschaften* **36**, 240 (1949).
- ⁷ G. L. Levinson, W. T. Simpson, and W. Curtis. *J. Am. Chem. Soc.* **79**, 4314 (1957).
- ⁸ E. G. McRae and M. Kasha. *J. Chem. Phys.* **28**, 721 (1958).
- ⁹ E. G. McRae and M. Kasha. In *Physical Processes in Radiation Biology*, p. 23. Academic Press, New York (1964).
- ¹⁰ A. Szent-Györgyi. *Science* **124**, 873 (1956).
- ¹¹ G. J. Hoijtink. *Z. Elektrochem.* **64**, 156 (1960).
- ¹² M. Kasha. *Rev. Mod. Phys.* **31**, 162 (1959).
- ¹³ M. Kasha. In *Physical Processes in Radiation Biology*, p. 17. Academic Press, New York (1964).
- ¹⁴ W. T. Simpson and D. L. Peterson. *J. Chem. Phys.* **26**, 588 (1957).
- ¹⁵ D. S. McClure. *Can. J. Chem.* **36**, 59 (1958).
- ¹⁶ M. Kasha. *Radiation Res.* **20**, 55 (1963).
- ¹⁷ W. Rhodes. *J. Am. Chem. Soc.* **83**, 3609 (1961).
- ¹⁸ M. Kasha, M. A. El-Bayoumi, and W. Rhodes. *J. Chim. Phys.* **58**, 916 (1961).
- ¹⁹ D. F. Bradley and M. K. Wolf. *Proc. Nat. Acad. Sci. U.S.* **45**, 944 (1959).
- ²⁰ D. S. McClure. *Can. J. Chem.* **36**, 59 (1958).
- ²¹ R. Coffman and D. S. McClure. *Can. J. Chem.* **36**, 48 (1958).
- ²² M. Kasha. *Discussions Faraday Soc.* No. 9, 14 (1950).
- ²³ P. Ramart-Lucas. In *Traité de Chimie Organique* (Ed. V. Grignard), Vol. II, p. 72. Masson et Cie, Paris (1936).
- ²⁴ G. Kortüm and G. Dreessen. *Chem. Ber.* **84**, 182 (1951).
- ²⁵ H. R. Rawls and M. Kasha. To be published.
- ²⁶ M. Kasha. *Light and Life* (Ed. W. D. McElroy and B. Glass), p. 31. Johns Hopkins Press, Baltimore (1961).

Note added in proof

All of the luminescence curves were determined at comparable settings of the spectrometer thus excluding simple quenching as an explanation of the phenomenon described in this paper.